

New Periodic Variables from the Hipparcos Epoch Photometry

Chris Koen¹ & Laurent Eyer^{2,3,4}

¹ South African Astronomical Observatory P O Box 9, Observatory, 7935 Cape, South Africa

² Instituut voor Sterrenkunde, Katholieke Universiteit Leuven, Belgium

³ Observatoire de Genève, 1290 Sauverny, Switzerland

⁴ Princeton University Observatory, Princeton, NJ 08544, USA

Accepted –. Received – ; in original form –

ABSTRACT

Two selection statistics are used to extract new candidate periodic variables from the epoch photometry of the Hipparcos catalogue. The primary selection criterion is a signal to noise ratio. The dependence of this statistic on the number of observations is calibrated using about 30 000 randomly permuted Hipparcos datasets. A significance level of 0.1% is used to extract a first batch of candidate variables. The second criterion requires that the optimal frequency be unaffected if the data are de-trended by low order polynomials. We find 2675 new candidate periodic variables, of which the majority (2082) are from the Hipparcos “unsolved” variables. Potential problems with the interpretation of the data (e.g. aliasing) are discussed.

Key words: methods: data analysis - methods: statistical - stars: variable

1 INTRODUCTION

The Hipparcos catalogues of variable stars (volumes 11 and 12 of ESA 1997) arose from the work of two groups, one at the Geneva Observatory and the other at the Royal Greenwich Observatory. Van Leeuwen (1997a) provided a brief summary of the variable star identification methods used by the two groups, while more detailed descriptions of the two independent strategies are available in Eyer (1998) and van Leeuwen et al. (1997). Although the variable star data have been widely used in studies of individual cases, or small collections of specific variables, little follow-up work with a global approach to the Hipparcos epoch photometry has been attempted since the release of the catalogues in 1997. One such study is the one by Koen (2001) who searched through the Hipparcos database for stars having multi-periodic behaviour.

Because of unavoidable statistical fluctuations, stars flagged as constant could in fact be variable, or even periodic, near the level of the precision of the Hipparcos measurements. The converse is inevitably also true, stars flagged as variable could be in reality constant stars at the Hipparcos precision. It is therefore important to have a sound evaluation of these contaminations.

The methodologies of the original analyses relied in the first instance on the estimated standard errors of the individual magnitudes. These errors were used for example in the

selection of variable stars, the determination of the limiting threshold to perform a period search, and the determination of the intrinsic amplitudes of the so-called unsolved variables (although details of the approaches taken by the two groups of analysts differed – see e.g. van Leeuwen 1997b). Indeed, not all stars flagged as variable were searched for a periodic behaviour – only those satisfying a criterion depending on the estimated amplitude, noise level and number of measurements were pursued. Such a criterion was set in order to minimize the number of variables with incorrect frequency determinations (due to aliasing). As noted by Eyer & Genton (1999), it is suspected that slight systematic shifts are present in the estimated standard errors, especially for the bright and faint ends of the catalogue.

The aim of the present study is to overcome the difficulties associated with the estimation of the variable star detection errors, first by tackling the problem from the outset by using Fourier methods, and second by estimating the type I errors without making assumptions about the nature of the data. The latter task is accomplished by determining the general statistical behaviour of the signal to noise ratio (section 2), which allows the computation of the expected number of spurious variables in a sample of candidate periodic stars. It therefore allows us to set numerical values on the Type I errors in order to keep these to an acceptable level.

We computed power spectra for, and fitted sinusoids to,

the observations of 30349 stars in order to calibrate our primary variable selection statistic, which is a signal to noise ratio. The test was then applied to the time series of 94336 stars out of a total of 118204 stars contained in the Hipparcos database. (Stars already flagged as periodic, and unflagged stars fainter than $V = 10$ were excluded from consideration).

The question of estimation of errors is not the only reason why the study we are presenting is of potential interest. Our method has the added advantages of considering the Hipparcos data from an entirely different viewpoint, and, of course, allows further extraction of relevant information from the photometric data.

The basic philosophies of the original studies and the present one are rather different. In the former, elimination of individual objects and an iterative approach were used: visual inspection of light curves and all phase diagrams, recalculation of periodic solutions on an individual basis and literature searches were done. The main aim of the original study was to produce statistically very well confirmed periodic variable stars. In this paper we develop simple but stringent criteria, and we publish the output as it stands, without eliminating any results, however unpalatable. Furthermore, it is clear that the scrutiny of individual stars which was carried out by the *Hipparcos* consortium (e.g. van Leeuwen 1997a) is not viable for large scale photometric surveys currently underway, or about to be begin. Fully automated algorithms, such as those proposed here, are needed to deal with star counts which may be several orders of magnitudes greater than in the case of *Hipparcos*.

The selection criteria are discussed in section 2. An alternative approach to the setting of significance levels is indicated in section 3. Results are given in section 4, and conclusions presented in section 5.

The interested reader is referred to ESA (1997), Eyer & Grenon (2000) and van Leeuwen (1997b), for discussions of quality and quality control of the *Hipparcos* epoch photometric data.

2 THE SELECTION CRITERIA

The primary variable selection criterion is based on the premise that the best-fitting sinusoid for a true variable ought to have a higher amplitude than would be the case for a constant star with a similar noise level and number of observations. Ideally, the test should be performed by, in a sense, comparing the data for a given star with itself, by using a permutation test. The latter is performed by noting that, under the null hypothesis the star is constant, all orderings of the observations in time are statistically equivalent. The test is then constructed by creating a large number of equivalent versions of the original dataset by randomly shuffling the observations, and comparing the amplitude of the best-fitting sinusoid to the original data, with the amplitudes of sinusoids fitted to shuffled data. If the true amplitude is sufficiently remarkable compared to the artificial amplitudes (e.g. if the true value is amongst the upper 0.1% of artificial values), the star may be considered a systematic variable. Such a permutation test is optimal in the sense that

it is completely true to life under the null hypothesis: the permuted datasets have the same time points of observation, and the same noise level, as the original data. There is but a single, but currently insurmountable, problem: the excessive amounts of computer time required to process the necessarily large number of replications of the original dataset. We therefore do what we consider the next best thing, which is to use the statistical properties of a large, representative sample for the Hipparcos database of stars, to produce a selection criterion which ought to work well in general.

The selection criterion is based on the signal-to-noise ratio R of the best-fitting sinusoid. The derivation of the exact form of the criterion is empirical, rather than theoretical. Calibration of the criterion is based on the results for three large sample datasets. In order to construct the latter, two non-overlapping sets of 10000 stars were randomly selected from the Hipparcos database. These lists were supplemented by a third consisting of all the apparently constant Hipparcos stars brighter than a magnitude limit of $V = 7$ (~ 10800 stars). The epoch photometry of each of the stars was extracted from the Hipparcos database. Suspect observations were removed in a two-step process: first, all measurements with Hipparcos flags larger than 7 were discarded. [Approximately 16% of the *Hipparcos* photometric observations are flagged, and 7.5% have flag values larger than 2. Generally speaking, the higher the flag value, the less reliable the observation (ESA 1997, Volume 3). Flag values less than 8 indicate that only one of the two *Hipparcos* consortia accepted the particular observations. Flag values greater than 7 indicate problems such as high background radiation, poor pointing, contamination by other stars, etc.] If fewer than $N = 20$ measurements remained, no analysis was attempted. Next, an iterative procedure was used to weed out outlying observations, by removing all values further than 2.58σ from the mean for that star. It is entirely possible that the latter step discards viable measurements (e.g. deep eclipses): however, the intention was to retain only *typical* observations, i.e. to eliminate observations which could exert undue influence on the results. Given the rather modest sizes of the datasets for some stars, single atypical observations can strongly affect results.

A periodogram was calculated for each dataset over the frequency interval $[0, 12] \text{ d}^{-1}$, as described in Koen (2001). The frequency corresponding to the periodogram maximum was noted, and a sinusoid with this frequency fitted to the data by linear least squares. The amplitude and phase of this sinusoid, together with the frequency, could then be used as starting guesses in a more sophisticated nonlinear least squares determination of the three quantities. The amplitude of the sinusoid and the standard deviation of the residuals were noted; the ratio R of the two is what we refer to as the “signal-to-noise ratio”.

A plot of the signal-to-noise ratio R against the number of observations N for all stars in each of the three samples shows an apparent power law dependence. It is therefore natural to examine the relationship between $\log R$ and $\log N$ (where “log” indicates natural logarithms in this section of the paper only): the relevant plots are in Fig. 1. Straight lines were fitted to each of the datasets in Fig. 1, and the results

are presented in Table 1. Datasets containing small numbers of observations ($N < 40$) were not taken into account, as the scatter for these is rather large; furthermore, low outlying observations in Fig. 1 ($\log R < -1.31$) were discounted. The parameters of the three lines agree quite well.

The results in Table 1 are for the model

$$\log R = a + b \log N$$

or equivalently

$$R = e^a N^b.$$

The implication is that

$$RN^{-b} = \text{constant}. \quad (1)$$

where the exponent b is in the range -0.468 to -0.460. Non-parametric regression estimates of the mean values of $RN^{0.465}$, which should be very close to being constant if (1) holds, are shown in Fig. 2. The method used to obtain the curves is known as “loess”, and consists in this instance of fitting locally linear estimates, with a window width of included data of 60% - see the brief discussion in Koen (1996), or the original papers by Cleveland & Devlin (1988) and Cleveland, Devlin & Grosse (1988). In order to avoid distortions caused by extreme points, data elements with $|RN^{0.465}| > 3$ were not taken into account; this meant the exclusion of respectively 16, 13 and 12 points for the three collections of datasets. The good qualitative agreement between the curves for the three different collections of data shows that the exponent b in (1) is not in fact perfectly constant. As will become clear, the variations of the order of 0.22 in the mean value of $RN^{0.465}$, for different N , could be of importance, and need to be taken into account. We therefore work with

$$R_1 = RN^{0.465} - M(N) \quad (2)$$

where $M(N)$ is the mean of the three loess curves in Fig. 2.

Fig. 3 contains plots of the statistics R_1 for each of the three collections of stars. It is unclear whether the larger scatter at smaller N is due to the larger number of data-points, or whether the variance of R_1 does in fact depend on N . Loess regressions of R_1^2 on N were therefore carried out, omitting the same outlying points as in the estimation of the mean. The results are given in Fig. 4. The agreement between the three curves is gratifying, and implies a rapid rise in the variance of R_1 as N decreases below 100. The final form of the signal-to-noise statistic is then

$$R_* = R_1/V^{1/2}(N) = V^{-1/2}(N) [RN^{-0.465} - M(N)] \quad (3)$$

where $V(N)$ is the mean of the three loess curves in Fig. 4. The standardised statistics R_* are plotted in Fig. 5.

The percentiles of R_* in Fig. 5 can now be used to produce critical values of this statistic. Of course, only the upper tail of the distribution is of interest in this context. The percentage points are in Table 2, where the results for each of the three individual collections of datasets are given for purposes of comparison; the last column of the Table shows the percentage points derived from all the data – these are the values used in what follows.

Inspection of the last column of Table 2 shows that

relatively small changes ~ 0.3 in R_* are associated with relatively large changes (factor ~ 2) in the significance levels of the statistic. This underlines the necessity for the standardisation of R into R_* .

One other very simple criterion is used to further weed out spurious variables. Many sets of observations have strong long-term trends, due to slow aperiodic brightness variations, which could give rise to prominent high frequency features in amplitude spectra through aliasing. It is therefore also required that the identified period satisfies

$$\Delta \equiv \frac{|P(\text{detrended}) - P(\text{raw})|}{\min[P(\text{detrended}), P(\text{raw})]} \leq 0.001 = \Delta_c.$$

The detrending is performed as described in Koen (2001); low order (≤ 3) polynomials are fitted to the data, and the fit with the highest significant order is used to prewhiten the data. Results are virtually identical for critical values Δ_c in the range 10^{-5} –0.005.

The results of applying the criteria are displayed in Table 3, which is based on selection with $R_* \geq 3.543$, i.e. the 0.1% critical value. There are three groups of stars: those classified as constant, or unclassified, in the Hipparcos catalogue; those classified as either “unsolved” or “microvariables”; and, for purposes of comparison, the Hipparcos “periodic” variables. It is instructive to consider results as a function of magnitude for the former group, and this is done in the Table, and now discussed. First, note that the numbers of candidate variables selected by the R_* criterion exceeds the expected number of spurious selections by factors of the order of 6.5–20 (although these numbers are misleading - see section 3). As expected, the percentage of variables decreases as the magnitude limit rises. For this reason it was decided not to extend the search beyond $V > 10$. Second, the Δ -criterion is obviously also quite stringent, particularly for the brighter stars. As an example of the influence of the precise value of Δ_c , we note that changing it to 10^{-5} would have removed one star from the final count in the top line in Table 3, while setting $\Delta_c = 0.005$ would have added four stars.

For the sake of completeness we mention that of the 593 new variables (i.e. stars in the first four lines of Table 3), 111 were classified as constant (designation “C”) in the Hipparcos catalogue, while 484 were unclassified (variability field blank).

There is an encouraging agreement with the results in the Hipparcos catalogue, in the sense that our R_* criterion recovers 86% of the Hipparcos periodic variables. It is also noteworthy that the Δ criterion eliminates only 16% of the periodic variables, the corresponding number for the unsolved variables being 56%.

The properties of the 371 Hipparcos periodic variables rejected by the R_* criterion were examined in some detail. Of these stars, 304 are eclipsing binaries. For 96 stars periods were not determined from the Hipparcos photometry [see the *Hipparcos Variability Annex* (ESA 1997, Volume 11)], while the periods of 5 are shorter than our limit of 0.08 d. In total 313 (i.e. 84%) of our non-detections fell in at least one of these categories. Of the remaining light curves, the vast majority exhibit some or other aberration: sparse phase coverage, low signal-to-noise, or unusual shapes (e.g. non-

monotonic changes on the ascending or descending branches, or flat-bottomed minima with relatively sharp maxima).

The variance of the Hipparcos photometric measurement errors was not constant with time (Eyer 1998), and thought should be given to the possible implications for the method described above. Since we have used an ordinary, rather than weighted, least squares algorithm, the only possible impact is through the initial frequency selection from the periodogram. It is now shown that the frequency dependence of the first two moments of the periodogram are unaffected by variability of the variance, and hence that the choice of “most likely” frequency is likewise unaffected.

Denote the deterministic (sinusoidal) signal by $f(t)$, and the measurement errors by $e(t)$, such that $Ee(t) \equiv 0$ and $\text{var}[e(t)] = Ee^2(t) = g(t)$, where $g(t)$ describes the time evolution of the photometric error variance. It follows that

$$S(\omega) = \frac{1}{N} \left| \sum_t [f(t) + e(t)] \exp(-i\omega t) \right|^2 = S_f(\omega) + S_e(\omega) \quad (4)$$

where $S(\omega)$, $S_f(\omega)$ and $S_e(\omega)$ are the periodograms of the observations, the deterministic process, and the measurement errors respectively. Now

$$\begin{aligned} ES_e(\omega) &= \frac{1}{N} \left[\sum_t Ee(t) \cos \omega t \right]^2 + \frac{1}{N} \left[\sum_t Ee(t) \sin \omega t \right]^2 \\ &= \frac{1}{N} \sum_t g(t) \end{aligned} \quad (5)$$

and

$$\begin{aligned} \text{cov}[S_e(\omega), S_e(\psi)] &= E[S_e(\omega) S_e(\psi)] - ES_e(\omega) ES_e(\psi) \\ &= \frac{1}{N^2} E \sum_t e^2(t) \sum_j e^2(j) \\ &\quad - \frac{1}{N^2} \left[\sum_t g(t) \right]^2 \\ &= \frac{1}{N^2} E \sum_t e^4(t) - \frac{1}{N^2} \left[\sum_t g(t) \right]^2 \end{aligned} \quad (6)$$

provided that measurement errors at different epochs are uncorrelated. If further $e(t)$ is independent of $f(t)$, the required result follows from (4)–(6).

3 QUALITY CONTROL BY ADJUSTMENT OF SIGNIFICANCE LEVELS

It is possible to adjust R_* according to the brightness of the stars studied, in order to obtain homogeneously reliable results. The approach is outlined below.

If all the stars were non-variable, the number selected by the R_* criterion would have had a binomial distribution: the probability of selecting k stars as variables, out of a sample of N stars, is

$$\text{Pr}(k) = \binom{N}{k} p^k (1-p)^{N-k}, \quad (7)$$

where p is the test level of R_* (e.g. $p = 0.001$ in Table 3). The numbers in column 3 of Table 3 are the expected values Np of spurious variables for the N given in column 1 of the Table. The probability of selecting *at least* K stars as variables is

$$\text{Pr}(k \geq K) = \sum_{k=K}^N \binom{N}{k} p^k (1-p)^{N-k}.$$

As an example, for the group of stars with $V \leq 7$ ($N = 10813$), the probabilities of selecting at least 11, 21 or 38 stars as variables are 0.52, 0.002, and 10^{-10} respectively. Clearly the probability of finding as many as 244 candidate variables by chance is minuscule, or, conversely, it is expected that most of the R_* -selected stars are truly variable.

The expected fraction η of spurious variable stars amongst the M candidate variables selected by the R_* criterion can be used as a measure of the quality of the collection of candidates. Conditionally on the value of M ,

$$\eta = \frac{Np}{M}.$$

The value of η for the four brightness intervals in Table 3 cannot be estimated from the numbers in the first four lines of the Table alone; it is necessary to include candidate variables from the ranks of the “unsolved” and “periodic” Hipparcos stars. The results are in Table 4, for three different significance levels of the R_* criterion.

Clearly candidate variables selected on the basis of sufficiently large R_* have good probabilities of being true variables: for example, with $\text{Pr}(R_*) < 0.001$, about 98 % of the faintest group of candidates are expected to be true variables. Nonetheless, the expected fraction of spurious variables could differ by a factor of three for stars of different brightnesses. This suggests adjusting R_* to obtain homogeneous results. For example, in order to have a uniform value of about 0.01 for η , $p = 0.002$ could be used for the brightest stars; $p = 0.001$ for the group with $7 < V \leq 8$; and $p = 0.0005$ for the stars fainter than $V = 8$.

A thorough implementation of such a “quality control” scheme obviously requires some further work, which is outside the scope of this paper. Nonetheless, it should be clear that it is one of the potential advantages of our variable selection methodology.

4 RESULTS

The pertinent results for the newly selected candidate periodic variable stars are presented in Table 5. Figs. 6a–e show an extract of the phase diagrams of our candidates. The 5 pages are each composed of the phased data for the first 36 stars in the first 5 groups in Table 3. Note that not all data points from the Hipparcos epoch photometry are plotted, but only those selected as explained in section 2.

The periodic annex of the Hipparcos catalogue contains 2712 variables, selected from a database of 118204 stars, giving a 2.3% incidence of periodic variables. In this study 2675 stars were selected from 94336 candidates. Of course, in order to compare this to the Hipparcos result, the information

in the last line of Table 3 should be incorporated, i.e. 4625 stars were selected from 97015 candidates, giving a percentage of 4.8. As already pointed out the current aim is not the same, hence the difference in results is not a cause for alarm.

Fig. 7 shows the period and amplitude distributions from Table 5, in the form of an amplitude-period plot; for comparison, Fig. 8 contains the corresponding results from the Hipparcos periodic variability annex. The locations of the Mira, Cepheid, RR Lyrae (ab and c types), and δ Scuti stars are clearly visible in the latter diagram.

In Fig. 7 we remark a strong accumulation of frequencies near 11.25 d^{-1} (2h 08 min), which was the rotation frequency of the satellite. These frequencies may be a cause for concern, although the results are in the correct range of periods and amplitudes for δ Scuti stars. A quick look at the spectral types of the stars confirms that many of the frequencies are probably spurious: for example, many M giant stars have periods in the suspect range. As mentioned before, there is a strong aliasing effect which is produced by convolution of low frequencies with the spectral window. Although the Δ -criterion of section 2 was designed to remove such variables, it is evidently not infallible. Furthermore, “real” variability in the data due to the rotation of the satellite remains a possibility: see Koen & Schumann (1999) where such an effect was shown to exist in Tycho epoch photometry. In fact, the referee of this paper has pointed out that errors in the modelling of the background radiation (in the case of fainter stars) or in the modelling of signal distortion (in the case of the brightest stars) may give rise to spurious 11.25 d^{-1} frequencies.

Table 6, which summarises the number distribution of variables in Table 5 as functions of frequency and spectral classification, throws further light on the aliasing problem. First, the number distribution is virtually constant for frequencies between 3 and 9.5 d^{-1} (see the last column in Table 6). The distribution increases sharply with higher frequencies, reaching a peak in the bin $[11, 11.5] \text{ d}^{-1}$. Second, in the frequency range $6-10 \text{ d}^{-1}$, the majority of stars are of spectral types A and F, and there are few late type stars. However, at higher frequencies, there is a substantial excess of late type (particularly M) stars.

The high incidence of A and F type stars at high frequencies is to be expected: these are the spectral types and frequencies associated with δ Scuti stars, which are known to be very abundant. By contrast, the large number of late type stars with high frequencies, is highly unexpected. There are two obvious explanations: either there is a substantial aliasing problem for these stars, or there is a class of rapidly variable late type stars which has been overlooked in the past. Choosing between these alternatives is beyond the scope of this paper.

We note in passing that of the 1112 stars with periods in excess of 4 d, only 43 have $P > 500$ d.

The authors are only aware of one theoretical investigation of the question of the correct determination of periods from *Hipparcos* data, namely Eyer et al. (1994). Those authors studied the range $0.03 < P < 1000$ d, and conclude that identifications are generally very accurate once the signal to noise ratio exceeds 1.25. The results of recent simula-

tion studies by ourselves support their findings. On the other hand, van Leeuwen et al. (1997) claimed that “...the sensitivity to detecting real periods in the range of a few days to 100 days is very low”. This is clearly a point deserving of further study.

There is an aggregation of points around amplitudes of the order of 0.04 mag, and periods of the order of 1.8 days, both in Fig. 7 and Fig. 8. Classification of the stars in Table 5 into different variable types is beyond the scope of this article, but looking at the spectral types, periods and amplitudes, it is noticeable that many different phenomena could be at work. Indeed, stars of the following types could be present: α Can Ven, SX Ari, γ Dor, α Cyg, γ Cas, BY Dra, FK Com, small amplitude red variables, eclipsing binaries of all types, and slowly pulsating B stars. We note in passing that, as could have been anticipated, most amplitudes are small: only 6.5% are larger than 0.1 mag. The smallest amplitude is 2.5 mmag.

In Fig. 9 finer detail such as an excess of periods near 57 days is visible. Now 56 days is the time interval during which the satellite rotation axis described one revolution on the cone on which it precessed. This seems to have generated an effect on the photometry of double stars, which is confirmed by the fact that the number of double star systems in the relevant histogram bin is substantially greater than in the adjacent bins. In the Fig. 9 histogram bin containing the 58 day period, the fraction of double stars is 23% (12 stars out of 53); by comparison the two lower adjacent bins, and the two higher adjacent bins, have double star fractions of 7% (4 stars out of 58) and 2% (1 star out of 45) respectively.

5 CONCLUSIONS

We conclude with some cautions: It is important to bear in mind the precise property the R_* statistic tests for, namely the existence of some frequency with which the data can be folded so that it shows an unusually large amplitude compared to the residual scatter. Although this will often mean that this frequency is truly present in the data, it will not always be the case. Both scatter in the measurements of constant stars, and fortuitous folding of the observations of non-periodic stars, can lead to the spurious identification of periodic variables, with data as sparse as those analysed here. Furthermore, the sparsity, and particular time distribution of the observations, imply that frequency aliasing is a substantial threat, so that all the identified frequencies should be treated with caution. In particular, inspection of Fig. 8 shows an excess of frequencies roughly in the range $10.5-11.5 \text{ d}^{-1}$, and it is well known (e.g. Eyer & Grenon 2000) that Hipparcos data are prone to aliasing of low frequencies to values near 11.2 d^{-1} .

On the other hand, for some Hipparcos datasets aliasing is, in practice, minimal, and frequencies can be determined more easily than would have been the case with typical groundbased observations - see, for example, the window function of HD95321 shown in Koen et al. (1999).

It must also be borne in mind that there are classes of periodic variables (e.g. δ Scuti stars) which commonly have frequencies beyond our detection limit of 12 d^{-1} . We will

either have failed to identify such stars as variables, or will have found aliases of the true frequencies.

Subject to all the above qualifications, we note that the value of the R_* statistic can be used to classify the candidates in order of "significance". In other words, this statistic renders possible a comparison between stars of different magnitudes and of different numbers of measurements.

REFERENCES

- Cleveland W.S., Devlin S.J., 1988, *J. Amer. Stat. Assoc.*, 83, 596
 Cleveland W.S., Devlin S.J., Grosse E., 1988, *J. Econometrics*, 37, 87
 ESA, 1997, The Hipparcos and Tycho Catalogues, ESA SP-1200.
 ESA Publications Division, Noordwijk
 Eyer L., Grenon M., Falin J.-L., Froeschlé M., Mignard F., 1994,
Solar Phys., 152, 91
 Eyer L., 1998, Ph.D Thesis, Geneva University
 Eyer L., Genton M.G., 1999, *A&AS*, 136, 421
 Eyer L., Grenon M., 2000, in Breger M., Montgomery M.H., eds,
ASP Conf. Ser. 210, *Delta Scuti and Related Stars*. Astron.
 Soc. Pacific, San Francisco, p. 482
 Koen C., 1996, *MNRAS*, 283, 471
 Koen C., Schumann R., 1999, *MNRAS*, 310, 618
 Koen C., Van Rooyen R., Van Wyk F., Marang F., 1999, *MNRAS*, 309, 1051
 Koen C., 2001, *MNRAS*, 321, 44
 van Leeuwen F., 1997a, in Perryman M.A.C., Bernacca P.L., eds.,
Hipparcos Venice '97. ESA, Noordwijk, p.19
 van Leeuwen F., 1997b, *Space Sci. Rev.*, 81, 201
 van Leeuwen F., Evans D.W., van Leeuwen-Toczko M.B., 1997,
 in Babu G.J., Feigelson E.D., eds., *Statistical Challenges in
 Modern Astronomy II*. Springer-Verlag, New York, p. 269

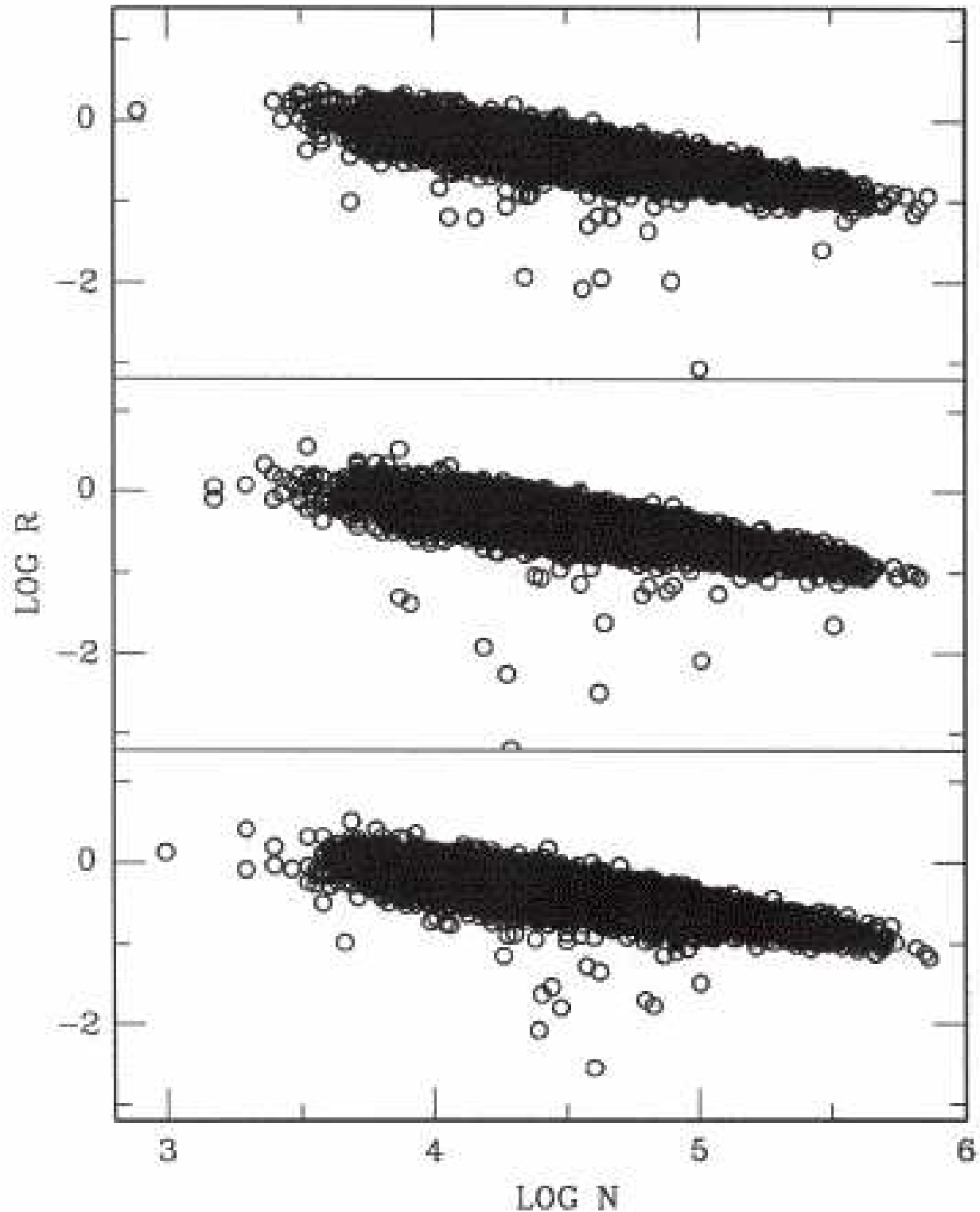


Figure 1. A log-log plot of the signal-to-noise ratio R against the number of accepted observations of each star, for each of the three collections of roughly 10000 stars.

Table 1. The results of fitting straight lines to each of the three datasets in Fig. 1. Only signal-to-noise ratios in excess of 0.27 ($\log R > -1.31$) and datasets containing at least 40 observations ($\log N > 3.69$) were taken into account in the fitting. Standard errors of the estimates are given in brackets.

Dataset	Intercept	Slope	<i>N</i>
1	1.71 (0.016)	-0.466 (0.0035)	9684
2	1.68 (0.016)	-0.460 (0.0036)	9732
3	1.72 (0.016)	-0.468 (0.0034)	10746

Table 2. Percentage points of the statistic R_* , for each of the three collections of stars, and for the three datasets combined.

Dataset	1	2	3	All
N	9747	9789	10813	30349
1%	2.56	2.59	2.55	2.566
0.5%	2.92	2.90	2.83	2.888
0.2%	3.44	3.24	3.24	3.282
0.1%	3.58	3.42	3.51	3.543

Table 3. Application of the selection criteria to stars classified as constant (or unclassified), and those classified as “unsolved” (or “microvariable”). The former group of stars has been subdivided according to brightness. The column headed “ $\text{Pr}(R_*) < 0.001$ ” shows the number of stars with $R_* > 3.543$ (the 0.1% point) from each grouping; the column headed “Final” are the numbers finally accepted as variables. Results for the Hipparcos “periodic” variables are also shown, for purposes of comparison.

Dataset	No. candidates	Expected spurious	$\text{Pr}(R_*) < 0.001$	$\Delta > 0.001$	Final
$V \leq 7$	10813	11	244	95	149
$7 < V \leq 8$	20149	20	224	77	147
$8 < V \leq 9$	34411	34	327	114	213
$9 < V \leq 10$	20134	20	154	70	84
Unsolved	7784		4396	2493	1908
Micro	1045		313	139	174
TOTALS:	94336		5658	2988	2675
Periodic	2679		2308	359	1949

Table 4. First page of the 2675 periodic candidate variable list.

HIP	V	FREQ	AMPL	N2	R	SpTy	H53
38	8.65	0.70787	0.0123	125	4.158	G6V	C
102	7.05	0.07586	0.0069	195	6.522	M1III	
274	6.24	0.34712	0.0166	130	6.261	B3Ia	U
279	8.69	0.61426	0.0155	128	5.990	B8V	
281	8.45	11.08512	0.0148	152	3.811	M0	U
283	7.45	6.16640	0.0133	88	5.313	A5	U
292	8.11	0.37690	0.0122	113	5.783	A0	U
355	4.99	11.22171	0.0053	132	4.968	K3Ibvar	M
457	7.47	0.00199	0.1044	172	19.893	M3III	U
458	6.97	11.44378	0.0081	99	4.911	K5	
519	7.92	1.47910	0.0740	119	7.687	F3IV	U
536	9.76	0.00361	0.2017	89	15.533	M6e	U
605	7.48	0.80210	0.0136	149	4.639	K5III	U
621	7.50	0.10826	0.0249	142	11.723	M1III	U
632	9.06	0.06260	0.0351	165	12.781	M2III:	U
690	9.26	0.05131	0.0143	134	3.736	G3/G5IV/V	
720	7.13	0.25630	0.0277	102	7.893	M2III	U
852	7.11	0.01851	0.0410	97	7.574	M4III:	U
893	7.78	0.03264	0.1070	101	10.773	M3III	U
926	7.47	0.08279	0.0080	130	5.620	K0	
949	8.09	0.55897	0.0094	195	4.308	B9	
967	6.18	0.73010	0.0058	153	4.786	K4III	M
970	7.80	11.65544	0.0202	160	7.867	M1III	U
989	7.69	0.31618	0.0732	126	14.190	M...	U
999	8.44	0.52745	0.0227	121	6.264	K0	U
1024	9.55	1.88707	0.0151	115	4.475	A5	
1035	8.84	0.52293	0.0100	149	3.657	F5	
1086	5.71	0.85784	0.0062	173	10.890	F0IV	M
1124	7.17	0.13408	0.0157	110	4.216	M4III:	U
1131	8.25	0.48166	0.0380	129	7.146	M2	U
1146	6.63	0.10180	0.0496	145	15.551	M1III	U
1158	5.13	0.45740	0.0213	66	7.372	M3IIIvar	U
1168	4.79	0.16767	0.0094	104	6.427	M2III	U
1191	5.77	2.49699	0.0077	75	3.958	B9V	M
1289	8.83	0.05126	0.0182	181	4.759	M0	U
1551	7.45	0.20012	0.0165	116	4.190	M3III	U
1555	7.78	0.04424	0.0422	153	21.399	M1III	U
1571	7.44	0.04682	0.0257	229	21.949	M1/M2III	U
1609	7.53	0.10716	0.0364	101	13.501	M0	U
1623	7.87	0.71752	0.0117	115	4.240	F6V	
1629	7.66	1.31813	0.0121	146	5.470	F2	U
1652	6.80	0.89264	0.0212	121	6.295	M2II:	U
1655	8.38	0.08694	0.0305	101	8.871	G5III	U
1763	8.76	0.26470	0.0256	61	4.051	M0	U
1792	7.94	0.17663	0.0215	73	5.145	G5	U
1843	9.99	0.78347	0.0251	97	3.682	M0	U
1880	7.70	11.72517	0.0267	155	8.822	M2III	U
1941	7.55	0.24823	0.0323	82	6.593	M...	U
1945	9.26	11.58187	0.0291	208	6.453	C4.5v	U
2086	6.24	0.08465	0.0153	86	3.589	M1III	U
2164	8.01	0.23288	0.0225	97	7.334	M2/M3III	U
2203	8.64	3.75862	0.0147	81	5.648	K2III	C
2219	5.01	0.21860	0.0830	67	14.094	M3IIIvar	U
2225	5.18	0.45460	0.0044	154	7.629	A2Vs	
2254	9.98	1.17703	0.0118	96	3.785	G2	
2283	7.35	0.58540	0.0182	91	6.738	K5III	U
2285	9.01	0.14403	0.0351	143	13.439	M0	U
2340	7.93	0.24137	0.0345	87	6.372	K2	U
2388	6.18	7.37913	0.0104	156	7.612	F2III	U
2474	6.18	0.92717	0.0068	137	4.190	B6V	M

Table 5. A check on the reliability of the R_* selection criterion: the parameter η is the expected percentage of false variables amongst the M selected stars. The numbers in column 2 refer to *all* Hipparcos stars in the particular magnitude interval.

Dataset	No. candidates	$p = 0.002$		$p = 0.001$		$p = 0.0005$	
		M	η	M	η	M	η
$V \leq 7$	13715	2371	1.16	2233	0.61	2119	0.32
$7 < V \leq 8$	22875	2129	2.15	1984	1.15	1860	0.61
$8 < V \leq 9$	37399	2208	3.39	2040	1.83	1888	0.99
$9 < V \leq 10$	21777	1149	3.79	1071	2.03	988	1.10

Table 6. The number distribution of the candidate variables in Table 5, as a function of frequency and spectral type. Classifications R, N, S and C are included in under M, while ‘‘Other’’ comprises primarily unclassified stars and composite spectra.

Frequency Interval	Spectral Type								Total
	O	B	A	F	G	K	M	Other	
[11.5, 12.0]	1	4	9	8	7	18	22		69
[11.0, 11.5]	2	15	12	7	6	39	63	5	149
[10.5, 11.0]	0	8	6	8	5	18	17	1	63
[10.0, 10.5]	0	6	3	4	5	5	3		26
[9.5, 10.0]	0	4	7	8	0	4	0		23
[9.0, 9.5]	0	4	6	4	0	1	0		15
[8.5, 9.0]	0	2	6	10	1	0	0		19
[8.0, 8.5]	0	0	2	6	1	0	0		9
[7.5, 8.0]	0	2	2	6	2	3	0		15
[7.0, 7.5]	0	1	1	7	2	0	0		11
[6.5, 7.0]	0	0	5	7	0	1	0		13
[6.0, 6.5]	0	1	5	9	0	0	0		15
[5.5, 6.0]	0	2	3	4	3	2	0		14
[5.0, 5.5]	0	3	1	5	3	4	0		16
[4.5, 5.0]	0	2	6	3	2	0	0		13
[4.0, 4.5]	0	4	3	3	0	0	0		10
[3.5, 4.0]	0	3	4	1	1	3	0		12
[3.0, 3.5]	1	7	3	4	1	1	0		17
[2.5, 3.0]	0	2	9	5	1	5	0		22
[2.0, 2.5]	0	11	9	6	4	6	0	1	37
[1.5, 2.0]	0	18	24	19	7	5	4		77
[1.0, 1.5]	0	57	34	21	6	13	30	4	165
[0.75, 1.0]	0	40	21	18	4	19	30	2	134
[0.50, 0.75]	0	57	33	19	9	35	72	4	229
[0.25, 0.50]	3	81	32	14	17	68	162	13	390
[0.00, 0.25]	5	117	59	35	73	243	550	30	1112

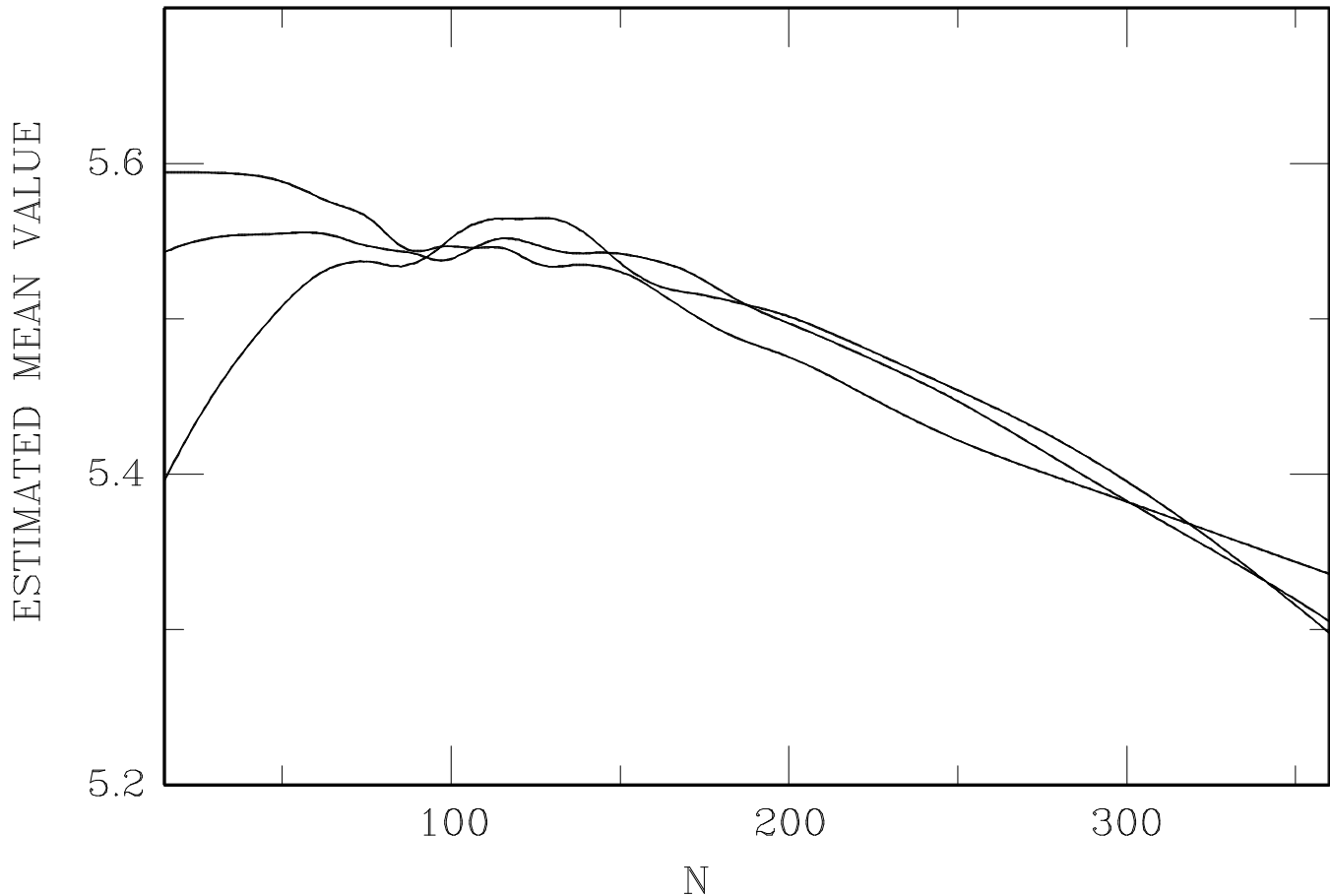


Figure 2. Non-parametric regression estimates of the means of $RN^{0.465}$, for each of the three collections of stars.

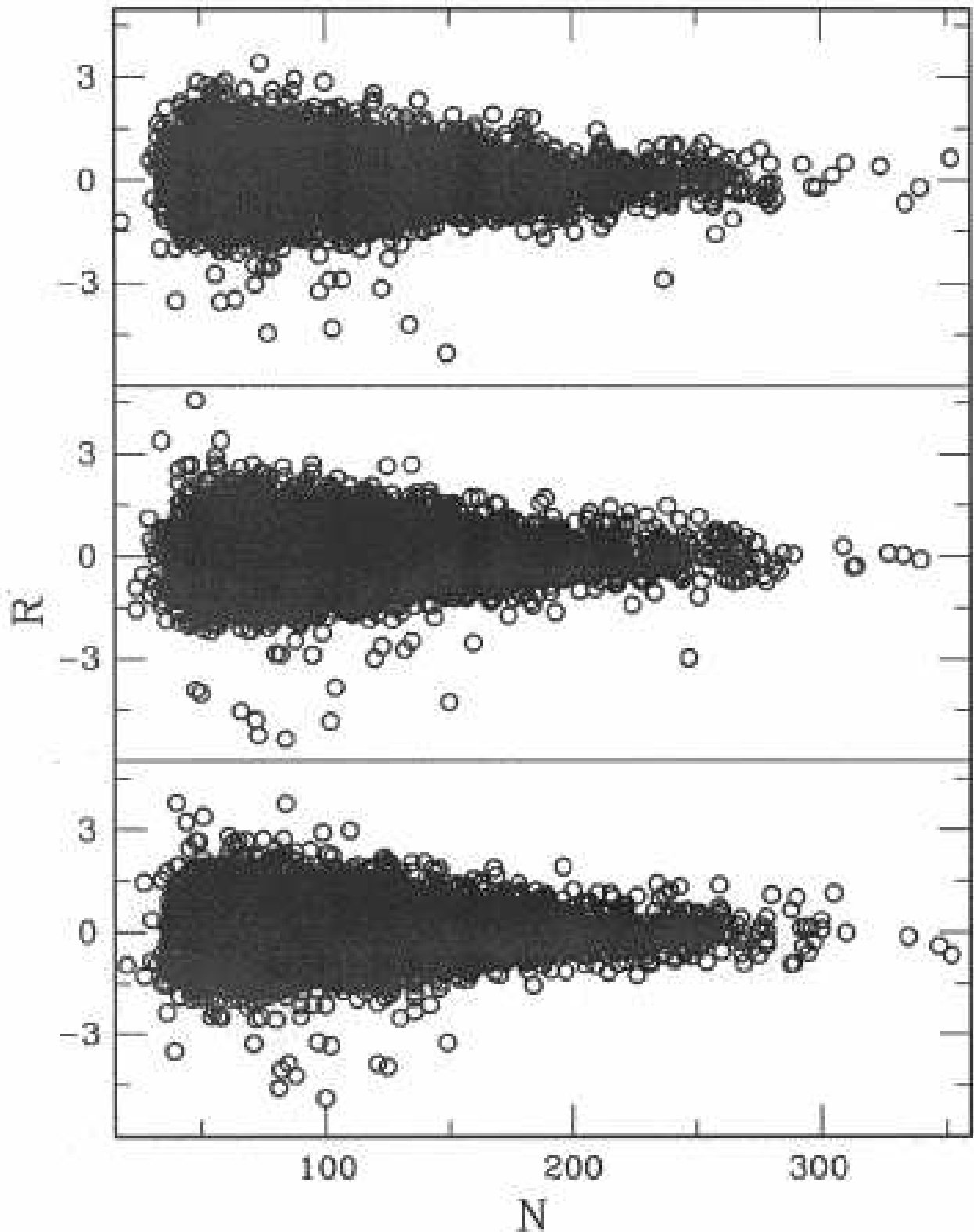


Figure 3. The statistic R_1 (see Eqn. (2)) for all stars in each of the three collections.

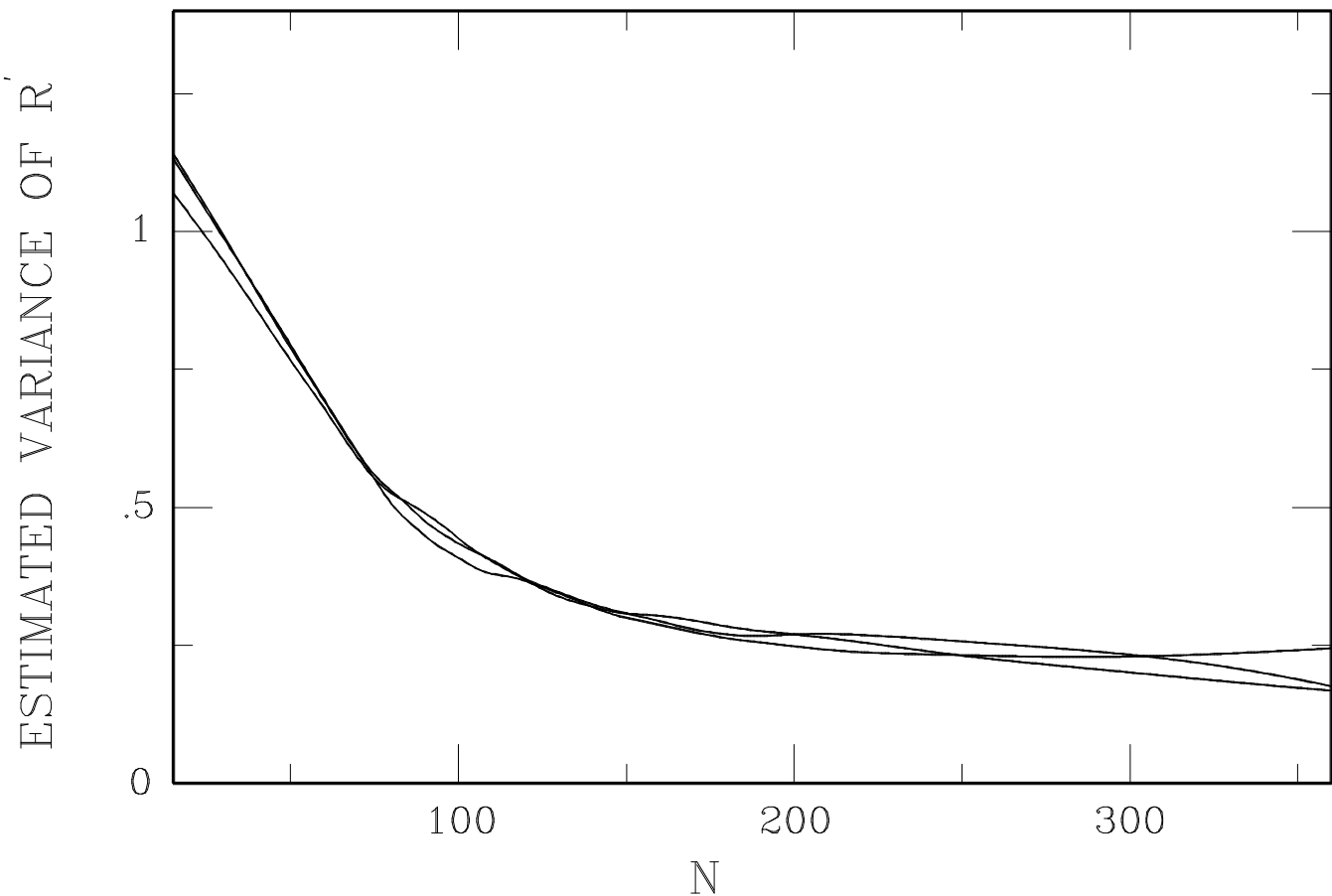


Figure 4. Non-parametric regression estimates of the variances of $RN^{0.465}$, for each of the three collections of stars.

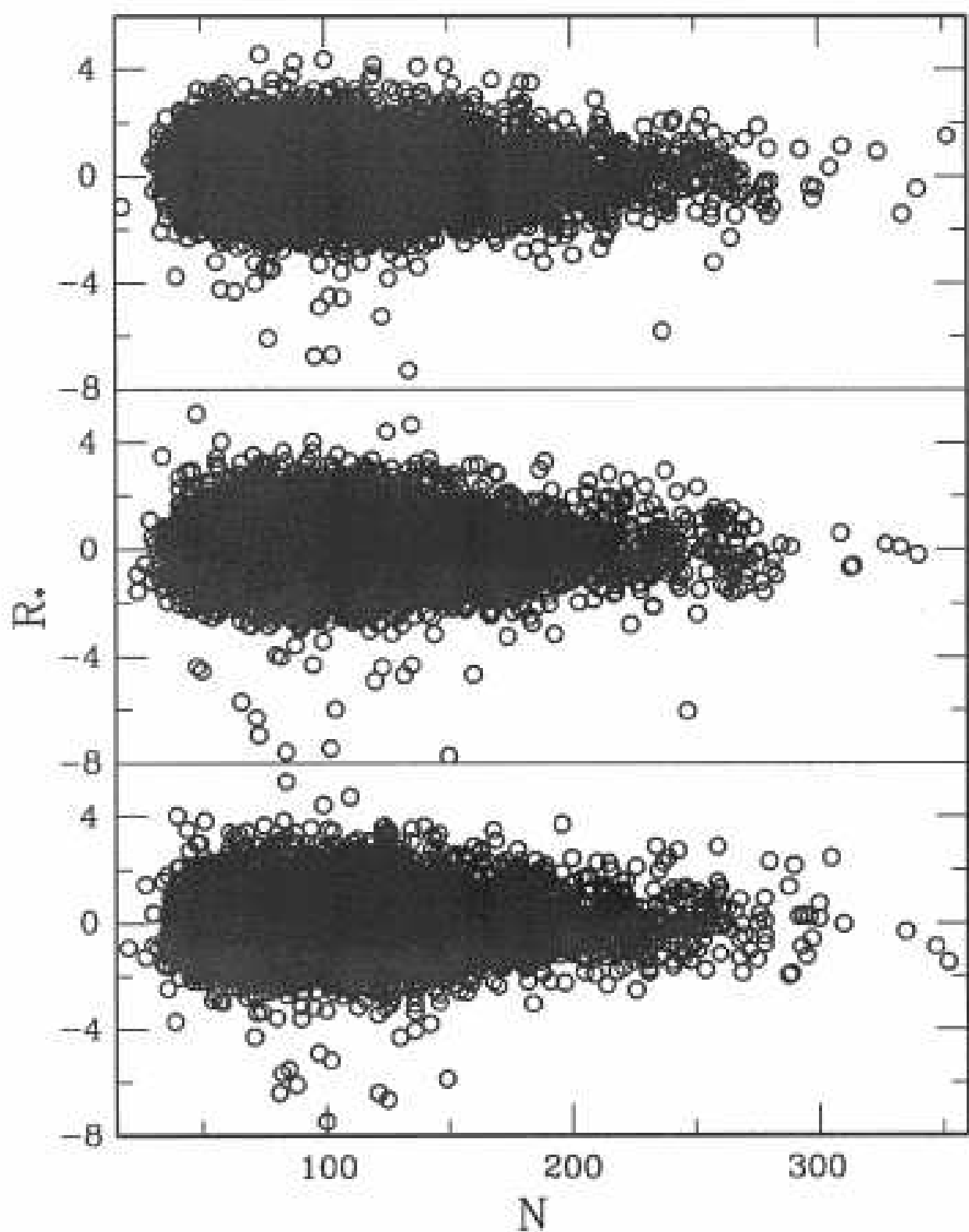


Figure 5. The statistic R_* (see Eqn. (3)) for all stars in each of the three collections.

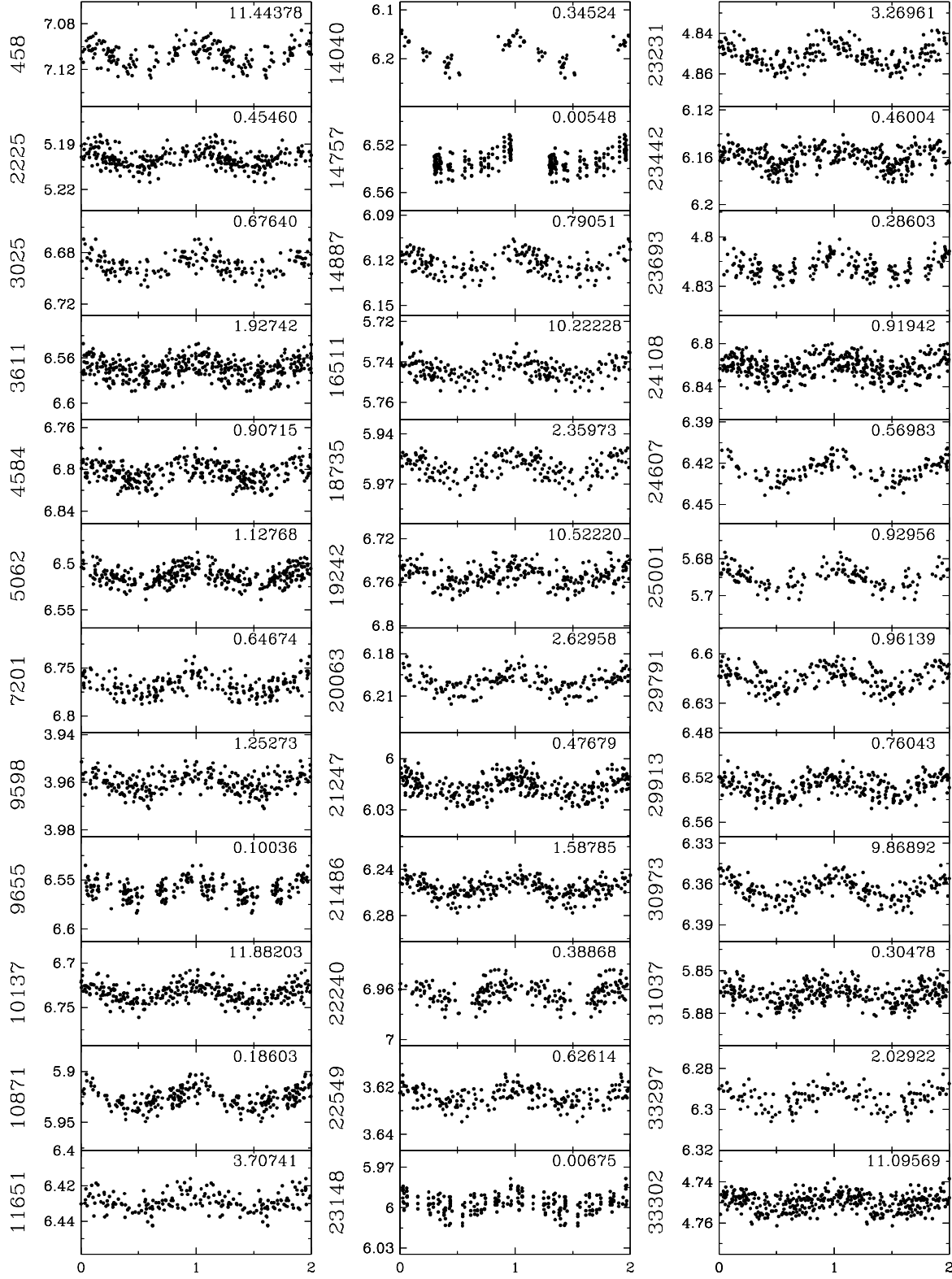


Figure 6. [Note: Only Fig. 6a is displayed here] Phased lightcurves for a sample of the candidate periodic variables in Table 5, for stars with $V \leq 7$ (a); $7 < V \leq 8$ (b); $8 < V \leq 9$ (c); $9 < V \leq 10$ (d); and for stars classified as ‘unsolved’ variables in the Hipparcos catalogue (e). The customary two cycles of variation are plotted.

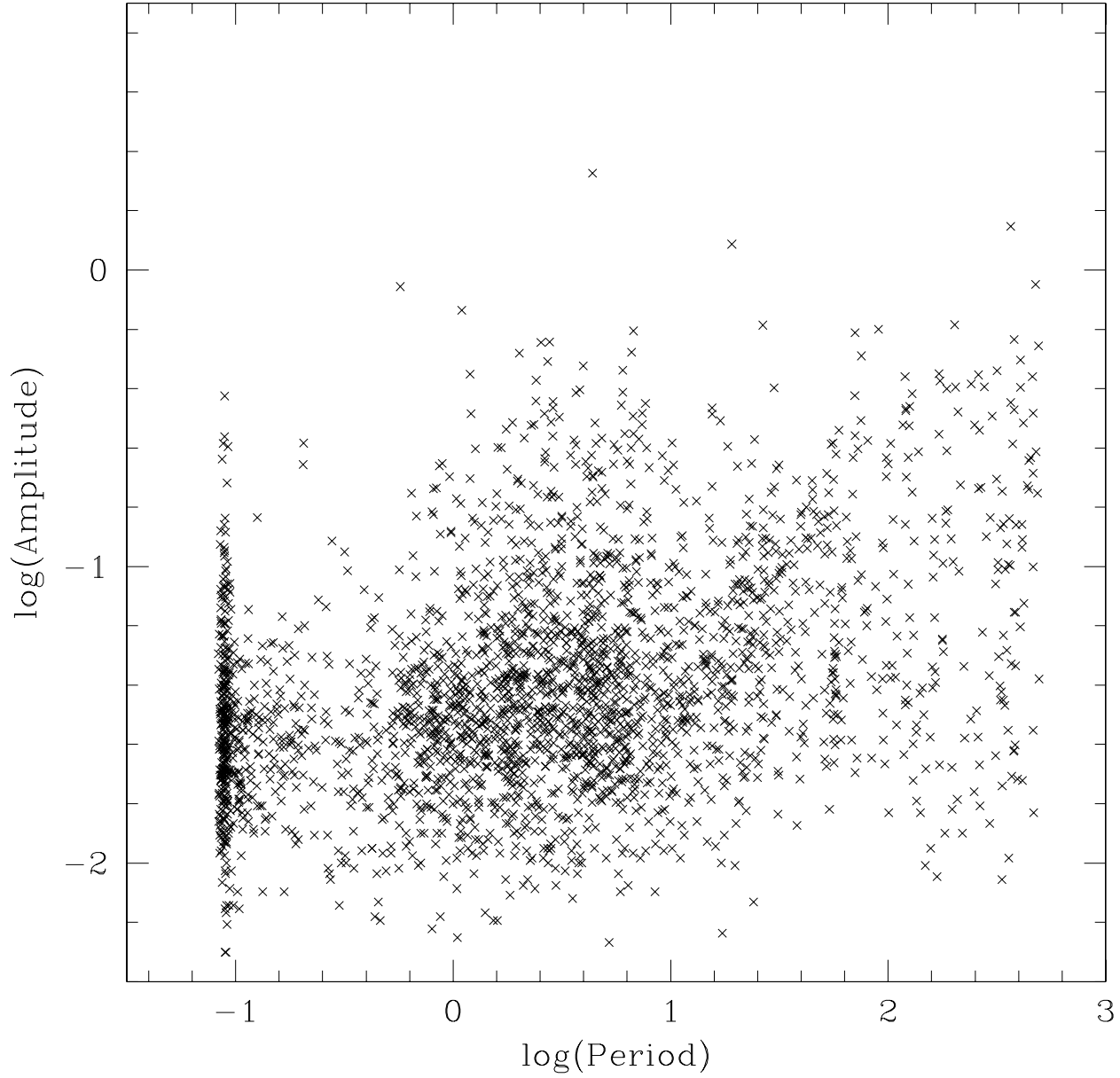


Figure 7. Amplitudes and frequencies of the new candidate variables in Table 5.

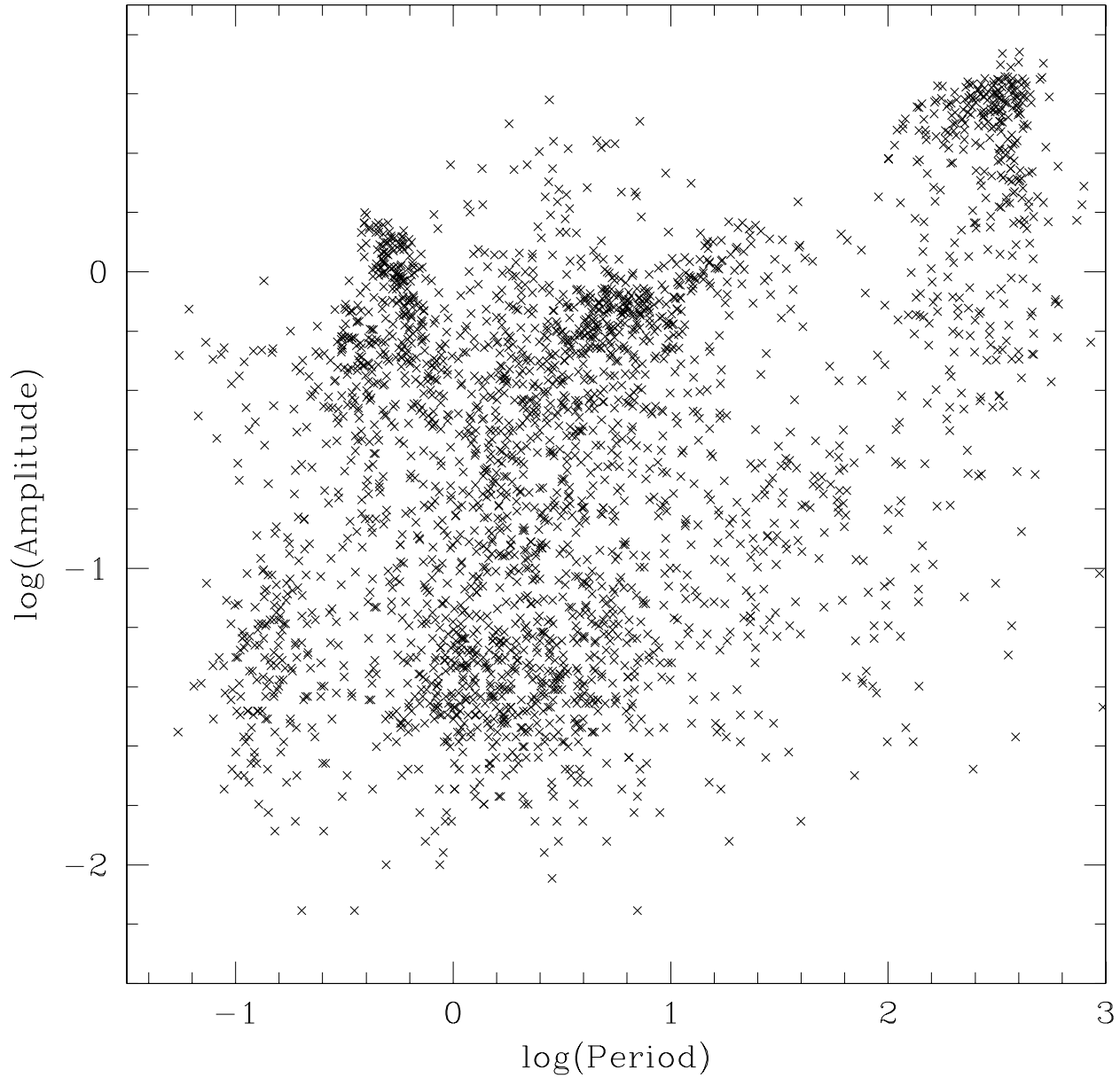


Figure 8. Amplitudes and frequencies of the Hipparcos periodic variables.

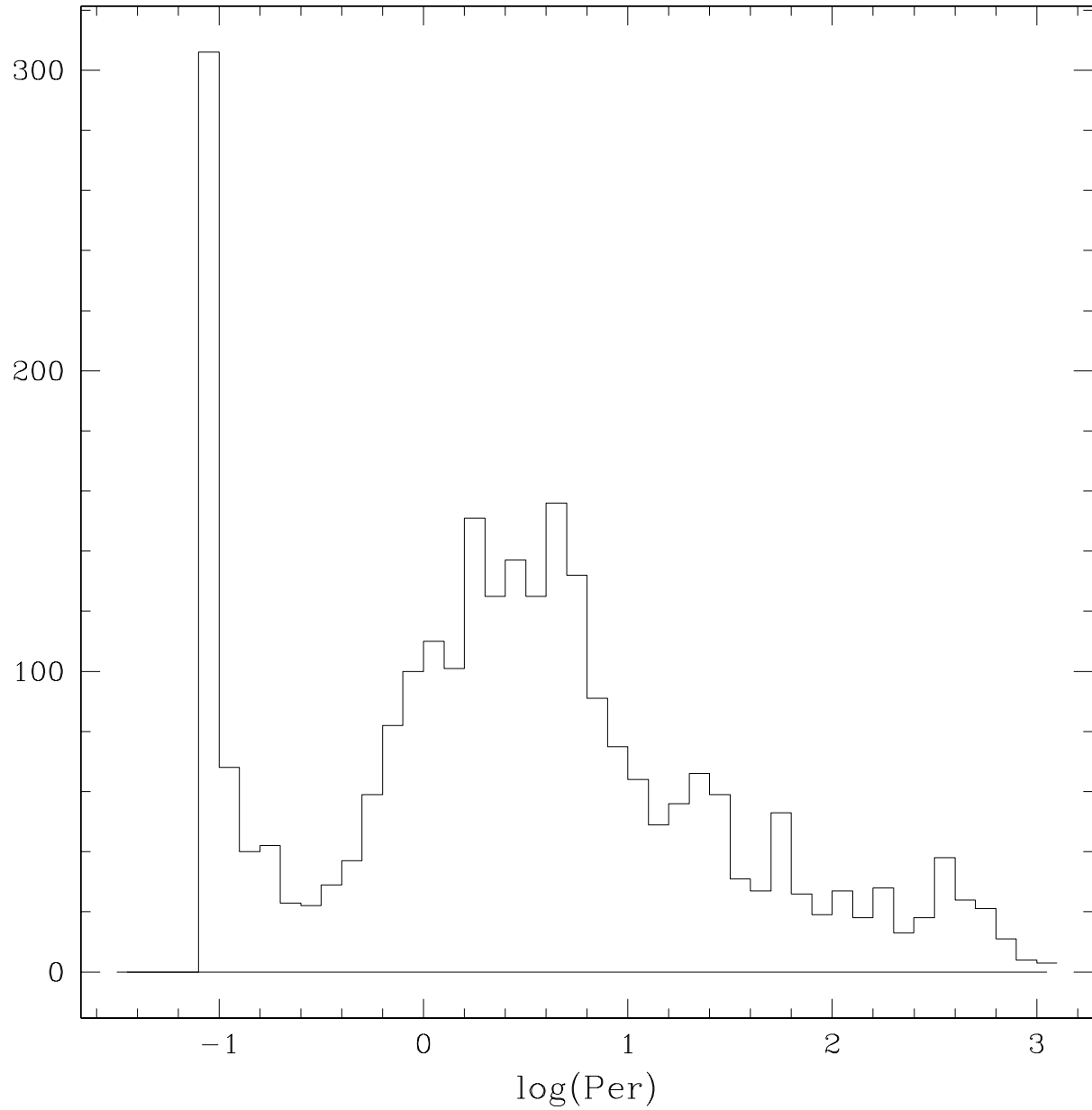


Figure 9. The distribution of the frequencies of the new candidate periodic variables in Table 5.